5126 *Inorg. Chem.* **2010**, *49*, 5126–5133
DOI: 10.1021/ic100252g

Inorganic Chemistry
Article

Cu^{II} Cross-Linked Antiparallel Dipeptide Duplexes Using Heterofunctional Ligand-Substituted Aminoethylglycine

Matthew B. Coppock, Matthew T. Kapelewski, Hye Won Youm, Lauren A. Levine, James R. Miller, Carl P. Myers, and Mary Elizabeth Williams*

Department of Chemistry, The Pennsylvania State University, 104 Chemistry Building, University Park, Pennsylvania 16802

Received February 7, 2010

Two artificial dipeptides containing both a pendant monodentate (pyridine (py)) and tridentate (terpyridine (tpy) or phenyl terpyridine (ϕ-tpy)) ligand on an aminoethylglycine (aeg) backbone have been synthesized. These oligopeptides are fully characterized by one and two-dimensional NMR spectroscopy, mass spectrometry, and elemental analysis. The ligands were chosen because they coordinate Cu^{2+} to form $[Cu(py)(tpy)]^{2+}$ complexes; when bound to the dipeptide scaffold, Cu^{2+} chelation cross-links the strands to form double-stranded duplex structures with an antiparallel arrangement. Using spectrophotometric titrations, we observe coordination of one Cu^{2+} metal per dipeptide strand. Mass spectrometry, NMR spectroscopy, vapor pressure osmometry, and HPLC confirm that the resulting structures are the dipeptide duplex cross-linked by two metal centers.

Introduction

An important aspect of designing potentially useful molecular materials for sensors, catalysis, artificial photosynthesis, and molecular wires that rival the utility and complexity of biological systems is the ability to control the placement of predetermined building blocks in specific geometries. Molecular recognition and self-assembly are commonly used to create complex supramolecular structures. For example, using modified DNA to direct the arrangement of functional species is of interest because sequence-specific base pairing produces well-defined double-stranded geometries that can be used as structural scaffolds. A key consideration in the molecular design of modified DNAs is to elicit recognition at precise locations, to induce folding into hairpin loops, or to place tags in specific positions with respect to each other. Modified DNA, for example, has been used to direct the assembly of two- and three-dimensional DNA lattices[1,2] and nanoparticle crystals.[3,4]

The insertion of electron donors and acceptors into oligonucleotides at well-defined locations has enabled the study of electron transfer in duplex DNA.[5] The substitution of natural base pairs with redox active species (e.g., inorganic complexes) is potentially useful for creation of molecular circuitry. Incorporation of multiple metal centers into the core of duplex DNA by replacement of nucleobases with bidentate ligands has been previously reported.[6] Heterometallic DNA structures based on differential coordination affinity to bidentate and monodentate ligands on the sugar phosphate backbone have recently been described.[7] Studies with the synthetic analogues peptide nucleic acid (PNA)[8] and glycol nucleic acid (GNA)[9] scaffolds similarly utilize pendant ligands to form metal coordinative cross-links. In each of these cases, metal insertion impacted the stability of the duplex; however molecular recognition was achieved in part by hydrogen bonding of complementary nucleobases.

*To whom correspondence should be addressed. E-mail: mbw@chem.psu.edu.

(1) Winfree, E.; Liu, F.; Wenzler, L. A.; Seeman, N. C. *Nature* **1998**, *394*, 539–544.
(2) Yan, H.; Park, S. H.; Finkelstein, G.; Reif, J. H.; LaBean, T. H. *Science* **2003**, *301*, 1882–1884.
(3) Nykypanchuk, D.; Maye, M. M.; van der Lelie, D.; Gang, O. *Nature* **2008**, *451*, 549–552.
(4) Park, S. Y.; Lytton-Jean, A. K. R.; Lee, B.; Weigand, S.; Schatz, G. C.; Mirkin, C. A. *Nature* **2008**, *451*, 553–556.
(5) (a) Lewis, F. D.; Wu, Y.; Zhang, L.; Zuo, X.; Hayes, R. T.; Wasielewski, M. R. *J. Am. Chem. Soc.* **2004**, *126*, 8206–8215. (b) Siegmund, K.; Daublain, P.; Wang, Q.; Trifonov, A.; Fiebig, T.; Lewis, F. D. *J. Phys. Chem. B* **2009**, *113*, 16276–16284. (c) O'Neill, M. A.; Dohno, C.; Barton, J. K. *J. Am. Chem. Soc.* **2004**, *126*, 1316–1317. (d) Genereux, J. C.; Barton, J. K. *Chem. Rev.* **2010**, *110*, 1642−1662.
(6) (a) Meggers, E.; Holland, P. L.; Tolman, W. B.; Romesberg, F. E.; Schultz, P. G. *J. Am. Chem. Soc.* **2000**, *122*, 10714–10715. (b) Atwell, S.; Meggers, E.; Spraggon, G.; Schultz, P. G. *J. Am. Chem. Soc.* **2001**, *123*, 12364–12367. (c) Tanaka, K.; Tengeiji, A.; Kato, T.; Toyama, N.; Shionoya, M. *Science* **2003**, *299*, 1212–1213.
(7) Tanaka, K.; Clever, G. H.; Takezawa, Y.; Yamada, Y.; Kaul, C.; Shionoya, M.; Carell, T. *Nat. Nanotechnol.* **2006**, *1*, 190–194.
(8) (a) Popescu, D.-L.; Parolin, T. J.; Achim, C. *J. Am. Chem. Soc.* **2003**, *125*, 6354–6355. (b) Watson, R. M.; Skorik, Y. A.; Patra, G. K.; Achim, C. *J. Am. Chem. Soc.* **2005**, *127*, 14628–14639. (c) Franzini, R. M.; Watson, R. M.; Patra, G. K.; Breece, R. M.; Tierney, D. L.; Hendrich, M. P.; Achim, C. *Inorg. Chem.* **2006**, *45*, 9798–9811.
(9) (a) Schlegel, M. K.; Zhang, L.; Pagano, N.; Meggers, E. *Org. Biomol. Chem.* **2009**, *7*, 476–482. (b) Schlegel, M. K.; Essen, L.-O.; Meggers, E. *J. Am. Chem. Soc.* **2008**, *130*, 8158–8159.

Published on Web 05/12/2010

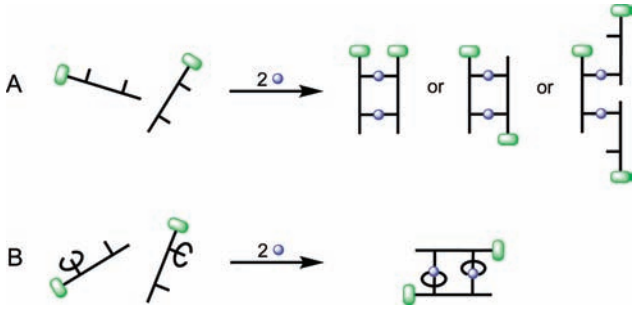

Figure 1. (A) Schematic of metal-induced duplex formation of a monofunctional, self-complementary dipeptide that can form parallel/antiparallel isomers and registers. (B) Schematic of metal coordination induced antiparallel duplex assembly of a heterofunctional, self-complementary dipeptide.

Previous work in our group has described the synthesis of artificial oligopeptides consisting of an aminoethylglycine (aeg) backbone with pendant ligands for the coordination to and cross-linking by transition metal ions.[10] The use of a neutral and flexible aeg backbone prevents the inherent electrostatic repulsion between anionic strands of DNA, precludes electrostatic attraction of metal cations to the backbone, has a broader range of solvent compatibility, and eliminates the irreversible oxidative electrochemistry of natural nucleic acids. Molecular recognition and duplex formation, which were first shown by Gilmartin et al.,[10a] are dependent solely on the robust metal to ligand bonds without reliance on nucleic acid hydrogen bonding. In these examples, the oligopeptides were substituted with repeating units of the same ligand (bpy or ϕ-tpy) on the aeg backbone. Although metal-coordination based self-assembly of double stranded duplexes was demonstrated, we recognized that both the parallel and antiparallel isomers were likely to form in solution. In addition, as the oligopeptide chains are lengthened to make larger and more complex architectures, there is increased possibility of chain misalignment and alternative register formation, as illustrated in Figure 1A. To combat these issues we have designed heterofunctional oligopeptides that mimic self-complementary sequences of DNA: the aeg dipeptide contains both pendant monodentate (pyridine) and tridentate (terpyridine or phenyl terpyridine) ligands. In the presence of a four-coordinate transition metal ion (e.g., Cu(II)) the ligands would be expected to coordinate two metals to gain coordinative saturation, forming the antiparallel dipeptide duplex depicted in Figure 1B. These dipeptide strands are the first self-complementary sequences containing two different ligands in our library.

In this initial study, we explore the use of this binding motif to form metal-linked dipeptide duplexes and describe the synthesis and characterization of two new heterofunctional artificial dipeptides. The purities of the Cu-containing dipeptides were confirmed by high performance liquid chromatography (HPLC), and the products identified using spectrophotometric titrations, vapor pressure osmometry, and mass spectrometry. These results are consistent with dipeptide duplexes each linked by two Cu(II) ions. These structures demonstrate a method for creating supramolecular inorganic complexes that imitate the molecular recognition of self-complementary DNA sequences, which improves control over the geometry of the duplex structures and points the way toward formation of larger and more complex architectures.

Experimental Section

Instrumentation and Analysis. Positive-ion electrospray mass spectrometry (ESI+) was performed at the Penn State Mass Spectrometry Facility using a Mariner mass spectrometer (Perseptive Biosystems). All NMR spectra were collected on 300, 360, or 400 MHz spectrophotometers (Bruker). UV−vis absorption spectra were obtained using a double-beam spectrophotometer (Varian, Cary 500). Elemental analysis was conducted by Galbraith Laboratories. Solution molecular weights were estimated using a Wespro Vapro model 5520 vapor pressure osmometer using 10−25 mmol/kg solutions in acetonitrile (ACN). A standard calibration curve was obtained using solutions of known concentration of tetrabutylammonium perchlorate in ACN.

Analytical-scale HPLC was performed with a Varian system equipped with two quaternary pumps (Model 210), an autosampler (Model 410), a UV−vis detector (Model 320), a fraction collector (Model 701), and a Thermo Scientific Betasil Silica-100 column (150 mm × 4.6 mm with 5 μm particle size). Dipeptides **3** and **4**, and their Cu(II)-containing products, were introduced in 5.0 μL injection size and analyzed using a flow rate of 0.4 mL/min. The eluent contained 0.1% trifluoroacetic acid (TFA) in a mixture of acetonitrile (ACN), water, and saturated aqueous potassium nitrate in a 6:3:1 volume ratio, respectively. Elution of the compounds was monitored at 264 nm.

Chemicals. All chemicals were reagent grade and used as received unless otherwise noted. *N*-hydroxybenzotriazole (HOBt) and 1-ethyl-3-(3-dimethylaminopropyl)carbodiimide hydrochloride (EDC) were purchased from Advanced ChemTech. O-Benzotriazole-*N*,*N*,*N*′,*N*′-tetramethyl-uronium-hexafluorophosphate (HBTU) was purchased from NovaBiochem. All other chemicals were purchased from Aldrich. 4′-Methyl-2,2′-bipyridine-4-acetic acid,[11] (4-[2,2′;6′,2″]terpyridin-4′-yl-phenyl)-acetic acid,[10d] fmoc-aeg-O*t*Bu·HCl,[12] fmoc-aeg(py)−OH·HCl,[10a] fmoc-aeg(bpy)-O*t*Bu,[13] fmoc-aeg(ϕ-tpy)-O*t*Bu,[10d] 4′-methyl-2,2′:6′,2″-terpyridine,[14] and pyridacyl pyridinium iodide[15] were synthesized as previously reported. Water was purified with a Nanopure water system (Barnstead, 18.2MΩ).

Synthesis. General Procedures for Peptide Deprotections. Briefly, a sample of fmoc-protected oligopeptide was stirred for 30 min in a 20% piperidine solution in acetonitrile. The reaction was extracted with hexanes (3 × 20 mL), and the acetonitrile layer was flash evaporated. The residue was dissolved in dichloromethane (30 mL) and flash evaporated twice, yielding the pure amine. Conversely, terminal acid formation was accomplished by deprotection of the *t*-butyl terminus of the oligopeptide using a 1:1 CF_3CO_2H/DCM mixture. The solution was stirred for 1 h at 25 °C, and the solvent flash evaporated. The residue was washed with Et_2O, resulting in the acid-terminated product.

(10) (a) Gilmartin, B. P.; Ohr, K.; McLaughlin, R. L.; Koerner, R.; Williams, M. E. *J. Am. Chem. Soc.* **2005**, *127*, 9546–9555. (b) Ohr, K.; Gilmartin, B. P.; Williams, M. E. *Inorg. Chem.* **2005**, *44*, 7876–7885. (c) Gilmartin, B. P.; McLaughlin, R. L.; Williams, M. E. *Chem. Mater.* **2005**, *17*, 5446–5454. (d) Ohr, K.; McLaughlin, R. L.; Williams, M. E. *Inorg. Chem.* **2007**, *46*, 965–974.

(11) Ciana, L. D.; Hamachi, I.; Meyer, T. J. *J. Org. Chem.* **1989**, *54*, 1731–1735.

(12) Thomson, S. A.; Josey, J. A.; Cadilla, R.; Gaul, M. D.; Hassman, C. F.; Luzzio, M. J.; Pipe, A. J.; Reed, K. L.; Ricca, D. J.; Wiethe, R. W.; Noble, S. A. *Tetrahedron* **1995**, *51*, 6179–6194.

(13) (a) Myers, C. P.; Gilmartin, B. P.; Williams, M. E. *Inorg. Chem.* **2008**, *47*, 6738–6747. (b) Myers, C. P.; Miller, J.; Williams, M. E. *J. Am. Chem. Soc.* **2009**, *131*, 15291–15300.

(14) Wolpher, H.; Sinha, S.; Pan, J.; Johansson, A.; Lundqvist, M. J.; Persson, P.; Lomoth, R.; Bergquist, J.; Sun, L.; Sundstrom, V.; Akermark, B.; Polivka, T. *Inorg. Chem.* **2007**, *46*, 638–651.

(15) Priimov, G. U.; Moore, P.; Maritim, P. K.; Butalanyi, P. K.; Alcock, N. W. *J. Chem. Soc., Dalton Trans.* **2000**, 445–449.

(4′-Methyl-2,2′:6′,2″-terpyridinyl)-acetic Acid (1). Using a modification of a previously reported synthesis,[16] an oven-dried flask was purged and refilled 3× with N_2, after which tetrahydrofuran (THF, 25 mL) was added. While the solvent was stirred at −15 °C, 2,2,6,6-tetramethyl piperidine (0.77 mL, 4.4 mmol) and methyl lithium (2.5 mL, 3.9 mmol) were added and the solution stirred for 15 min. A deaerated solution of 4′-methyl-2,2′:6′2″-terpyridine (0.87 g, 3.5 mmol) dissolved in a minimal amount of THF was added and stirred for 30 min. CO_2 (g) was then bubbled into the reaction for 1 h. The resulting solid was collected and dissolved in 1 M HCl (20 mL). Ethanol (EtOH, 30 mL) was added to the solution, and the solvent volume was reduced via flash evaporation until a brown solid began to precipitate. After cooling in the freezer overnight, a brown solid was collected. Yield = 400 mg (40%). ^{1}H NMR (400 MHz, DMSO-d_6): δ 8.97 (s, 4H); 8.68 (s, 2H); 8.54 (t, J = 6 Hz, 2H); 7.95 (t, J = 6 Hz, 2H); 3.98 (s, 2H).

Fmoc-aeg(tpy)-O*t*Bu (2). A solution of compound **1** (0.300 g, 1.0 mmol), EDC (0.20 g, 1.0 mmol), HOBt (0.14 g, 1.0 mmol), and DIPEA (0.52 mL, 3.2 mmol) in DCM (50 mL) was stirred at 0 °C for 15 min. The mixture was added to fmoc-aeg-O*t*Bu (0.34 g, 0.79 mmol) dissolved in DCM (25 mL) and stirred at 25 °C for 48 h. The solution was extracted with water (3 × 30 mL), and the aqueous fractions were combined and back-extracted with DCM (25 mL). The organic solutions were combined and dried over solid Na_2SO_4. Solvent was removed via flash evaporation, resulting in a yellow oil which was purified on a silica gel column eluting with a solvent gradient (100% DCM to 5% MeOH in DCM). The first yellow band was collected, like fractions were combined, and the solvent removed under vacuum yielding a yellow solid. Yield = 394 mg (75%). ^{1}H NMR (400 MHz, chloroform-d): δ 8.64 (d, J = 9 Hz, 2H); 8.56 (d, J = 9 Hz, 2H); 8.33 (s, 1H); 8.31 (s, 1H); 7.90−7.78 (m, 2H); 7.67 (d, J = 7 Hz, 2H); 7.58 (m, 2H); 7.40 (t, J = 7 Hz, 2H); 7.34−7.27 (m, 4H); 4.44 (d, J = 7 Hz, 1H); 4.33 (d, J = 7 Hz, 1H); 4.25 (t, J = 7 Hz, 1H); 4.07−3.83 (m, 4H); 3.68−3.62 (m, 2H); 3.53 (m, 1H); 3.28 (m, 1H); 1.48 (s, 9H). MS (ESI+) $[M + H]^+$ Calcd 670.7, Found 670.4.

Fmoc-aeg(py)-aeg(tpy)-O*t*Bu (3). The fmoc was cleaved from compound **2** using the above protocol, giving aeg-(tpy)-O*t*Bu. A mixture of fmoc-aeg(py)-OH (0.30 g, 0.61 mmol), EDC (0.12 g, 0.61 mmol), HOBt (0.082 g, 0.61 mmol), and DIPEA (0.31 mL, 1.9 mmol) was suspended in DCM (60 mL) and allowed to stir for 15 min at 0 °C. The solution was added to aeg-(tpy)-O*t*Bu (0.21 g, 0.47 mmol) dissolved in DCM (15 mL) and stirred at 25 °C for 48 h. The reaction was extracted with water (3 × 30 mL), the aqueous fractions combined and back-extracted with DCM (20 mL). The combined organic fractions were dried over Na_2SO_4, and the solvent was flash evaporated to give a light orange solid. The solid was purified by chromatography on a silica gel column eluting a solvent gradient (100% DCM to 5% MeOH in DCM). Like fractions were combined and flash evaporated to yield a light orange solid. Yield = 170 mg (41%). ^{1}H NMR (400 MHz, chloroform-d, Supporting Information, Figure S2): δ 8.67−8.61 (m, 2H); 8.58 (d, J = 7 Hz, 2H); 8.39 (d, J = 6 Hz, 2H); 8.33 (s, 2H); 7.89−7.81 (m, 2H); 7.73 (d, J = 8 Hz, 2H); 7.66−7.50 (m, 2H); 7.37−7.27 (m, 6H); 7.06 (d, J = 6 Hz, 2H); 4.41−4.30 (m, 2H); 4.24−4.11 (m, 1H); 4.07−3.90 (m, 4H); 3.90−3.65 (m, 4H); 3.65−3.45 (m, 4H); 3.45−3.22 (m, 4H); 1.47 (s, 9H). HR MS (ESI+) $[M + H]^+$ Calcd 889.3969, Found 889.4037. Elemental Anal. **fmoc-aeg(py)-aeg(tpy)-O*t*Bu·H_2O** Calc: 67.53 C; 6.00 H; 12.35 N; Found: 67.3 C; 6.00 H; 12.2 N.

Fmoc-aeg(py)-aeg(ϕ-tpy)-O*t*Bu (4). The fmoc was cleaved from fmoc-aeg-(ϕ-tpy)-O*t*Bu using the above procedure, giving aeg-(ϕ-tpy)-O*t*Bu. A mixture of fmoc-aeg(py)-OH(0.27 g, 0.801 mmol), EDC (0.15 g, 0.801 mmol), and HOBt (0.10 g, 0.801 mmol) was suspended in DCM (35 mL) and allowed to stir for 15 min at 0 °C. To this, DIPEA (0.38 mL, 2.20 mmol) was added, and the reaction was stirred for 1 h at 0 °C. This was then transferred to the solution of aeg-(ϕ-tpy)-O*t*Bu (0.30 g, 0.66 mmol) in DCM (15 mL), and the mixture was stirred for 48 h at 25 °C. The solution was extracted with water (3 × 20 mL), the aqueous fractions combined and back-extracted with DCM (20 mL). The organic layer was dried over Na_2SO_4, separated from the drying agent, and flash evaporated to give a yellow oil. The oil was chromatographed on a silica gel column, eluting with a solvent gradient (100% DCM to 10% MeOH in DCM). Like fractions were combined, and the solvent was removed under vacuum to yield a yellow solid. Yield = 213 mg (38.3%). ^{1}H NMR (360 MHz, chloroform-d, Supporting Information, Figure S7): δ 8.73−8.67 (m, 4H); 8.65 (d, J = 7 Hz, 2H); 8.44 (d, J = 5 Hz, 2H); 7.91−7.80 (m, 4H); 7.71 (d, J = 8 Hz, 2H); 7.55 (d, J = 8 Hz, 2H); 7.40 (d, J = 7 Hz, 2H); 7.36−7.33 (m, 4H); 7.29−7.20 (m, 2H); 7.11 (d, J = 5 Hz, 2H); 4.40−4.25 (m, 2H); 4.22−4.10 (m, 1H); 4.07−3.88 (m, 4H); 3.88−3.71 (m, 4H); 3.71−3.54 (m, 4H); 3.54−3.30 (m, 4H); 1.47 (d, 9H). HR MS (ESI) $[M + H]^+$ Calcd 964.4339, Found 964.4350. Elemental Anal. **fmoc-aeg(py)-aeg(ϕ-tpy)-O*t*Bu·H_2O** Calc: 69.64 C; 5.95 H; 11.40 N. Found: 69.51 C; 5.95 H; 11.41 N.

General Procedure for Reaction and Isolation of Cu(II) Complexes. A solution of the peptide was prepared in MeOH and combined with a solution containing a slight molar excess of $Cu(NO_3)_2 \cdot 2.5H_2O$, stirred, and heated at 40 °C for 24 h. The solvent was removed under reduced pressure, and the solid was dissolved in a 1:4 MeOH/H_2O solution. A saturated solution of NH_4PF_6 was added, producing a blue to green precipitate. The solid was collected by filtration and rinsed with H_2O and Et_2O. **[Cu_2(3)$_2$](PF_6)$_4$** MS (ESI) (Figure 3, Supporting Information, Figure S14) $[[Cu_2(\mathbf{3})_2](PF_6)_2]^{2+}$ calcd 1097.3, found 1097.3; $[[Cu_2(\mathbf{3})_2](PF_6)]^{3+}$calcd 683.2, found 683.2. ^{1}H NMR (400 MHz, ACN-d_3, Supporting Information, Figure S12): δ 7.90−7.25 (br m, 16H); 4.40−2.10 (br m, 38H); 1.35 (br s, 18H). **[Cu_2(4)$_2$](PF_6)$_4$** MS (ESI) (Figure 3, Supporting Information, Figure S15) $[[Cu_2(\mathbf{4})_2](PF_6)_2]^{2+}$ Calcd 1173.3, found 1173.4; $[[Cu_2(\mathbf{4})_2](PF_6)]^{3+}$ Calcd 733.9, found 734.0. ^{1}H NMR (400 MHz, ACN-d_3, Supporting Information, Figure S13): 8.00−7.25 (br m, 24H); 4.60−2.55 (br m, 38H); 1.45 (br s, 18H).

Spectrophotometric Titrations. Titrations were performed using methanolic solutions of known concentrations of mono- or dipeptide and $Cu(NO_3)_2$. For measurements of visible wavelength absorption, ~10 mM peptide solutions were used; in the UV region, solutions of ~10 μM peptide were used. Solutions were background subtracted using the double beam of the spectrometer. Titrations either incrementally added metal ion to peptide solution or peptide to metal ion solution, as indicated below.

Results and Discussion

Synthesis and Characterization of Artificial Dipeptides. Incorporation of a tridentate ligand, in this case terpyridine or phenyl terpyridine, in series with the monodentate ligand pyridine onto the aminoethylglycine (aeg) scaffold creates a bifunctional peptide with variable affinity for metal ions. To coordinatively saturate Cu(II), the tridentate tpy and monodentate py ligands are expected to form $[Cu(tpy)(py)]^{2+}$ complexes in a distorted square planar geometry.[17] Thus, the motif for molecular recognition to form an antiparallel dipeptide duplex uses ligands with coordinatively "complementary" denticities with respect to the tetracoordinate metal ion: the dipeptides have been designed to self-assemble into duplexes

(16) Potts, K. T.; Usifer, D. A.; Guadalupe, A.; Abruna, H. D. *J. Am. Chem. Soc.* **1987**, *109*, 3961–3967.

(17) Su, C.-C.; Li, C.-B. *Polyhedron* **1994**, *13*, 825–834.

Scheme 1. Terpyridine Monomer Synthetic Strategy; (i) HBTU, HOBt, DIPEA; (ii) 20% Piperidine in ACN

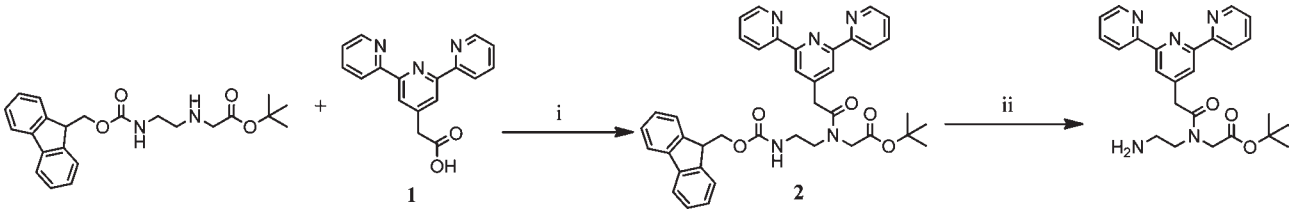

Scheme 2. Dipeptide Synthetic Strategy; (i) EDC, HOBt, DIPEA

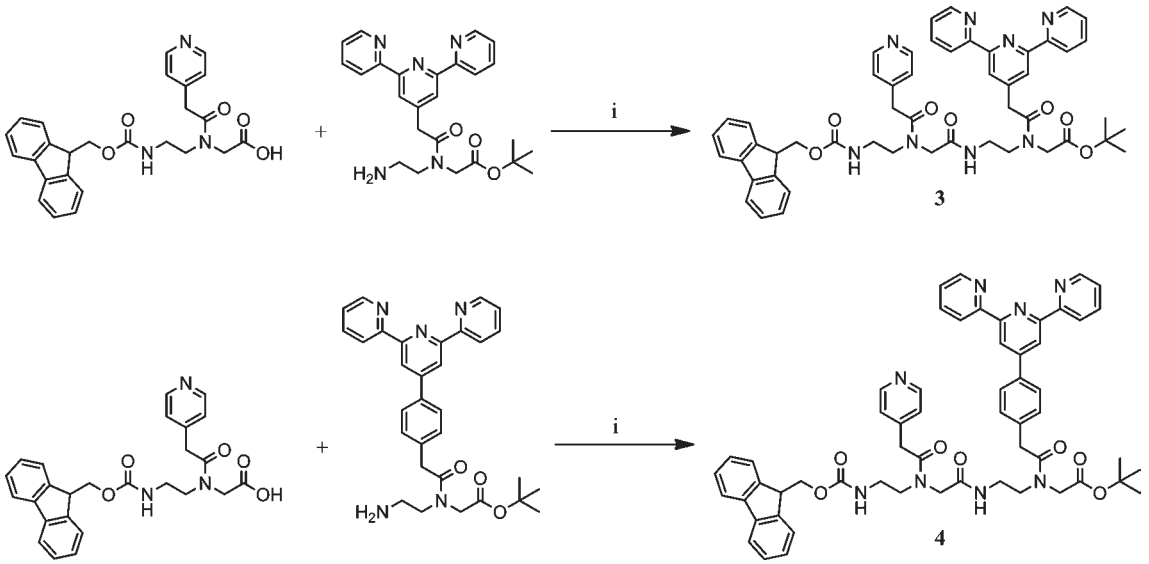

upon chelation with tetracoordinate metals such as Cu(II). The two tridentate ligands selected for these studies have differing length attachments to the backbone, which would impact the relative locations of the Cu cross-links (vide infra).

The termini of the aminoethylglycine backbone have been protected with fmoc and *t*-butyl ester as in previous studies.[10] Since the fmoc group is base labile and the *t*-butyl ester group is acid labile, selective deprotection followed by extension of the peptide chain was achieved from both termini. Solution phase synthesis of these dipeptides was used to enable bidirectional chain lengthening in future studies as well as to increase yields compared to solid phase synthesis. The purification techniques used in solution based synthesis allow for isolation of greater amounts of product than solid phase methods.[10a]

For the synthesis of a dipeptide with pendant pyridine and either terpyridine or phenyl terpyridine ligands, fmoc-aeg(py)-O*t*Bu and fmoc-aeg(ϕ-tpy)-O*t*Bu monomers were prepared according to previous work.[10b,d] Analogously, terpyridine acetic acid was prepared using modified syntheses and coupled to the aeg backbone with our standard conditions (Scheme 1).[10d] The fmoc protecting group was selectively removed from the tridentate monomers under mild basic conditions, resulting in primary amine termini. This method was chosen to reduce the aromatic bulkiness of the monomers and maximize the coupling yield. Shown in Scheme 2, the tridentate monomers (aeg(tpy)-O*t*Bu or aeg(ϕ-tpy)-O*t*Bu) were separately combined with acid-terminated pyridine monomer (fmoc-aeg(py)-OH) and EDC/HOBt coupling reagents. In both cases, the dipeptide product was purified by column chromatography, and purity assessed by HPLC: Figure 2 contains the chromatograms of dipeptides **3** and **4** (red lines), which have a single, sharp peak indicative of a single, pure species. Additional confirmation of purity by elemental analysis, and identity by NMR spectroscopy and positive ion electrospray mass spectrometry (vide infra), are used to fully characterize the dipeptides. The overall reactions produced 41% yield for fmoc-aeg(py)-aeg(tpy)-O*t*Bu (**3**) and 38% yield for fmoc-aeg(py)-aeg(ϕ-tpy)-O*t*Bu (**4**) dipeptides, both of which are higher yields and in larger quantities than those obtained for the solid-phase peptide synthesis of ϕ-tpy substituted dipeptides (i.e., 23%).[10d]

The ^{1}H NMR spectra of the dipeptides yielded the anticipated relative proton integrations (i.e., 9 *t*-butyl protons, 18 aliphatic protons, and 22 aromatic protons for dipeptide **3**, and 9 *t*-butyl protons, 18 aliphatic protons, and 26 aromatic protons for dipeptide **4**). The protons assigned to the fmoc protecting group, as well as the pyridine ligand, appear at the same positions in both NMR spectra (see Supporting Information, Figures S2 and S7). Protons on the heterocyclic terpyridine ring in each of the tridentate ligands have similar resonances, but the phenyl ring shifts the terpyridine protons slightly downfield, whereas proximity to the backbone shifts these slightly more upfield in dipeptide **4**.

Structural characterization of the dipeptides was therefore further confirmed using ^{1}H$-^1$H COSY, ^{13}C$-^1$H HMQC, and ^{13}C$-^1$H HMBC. The COSY spectra clearly show the couplings between aromatic protons and between

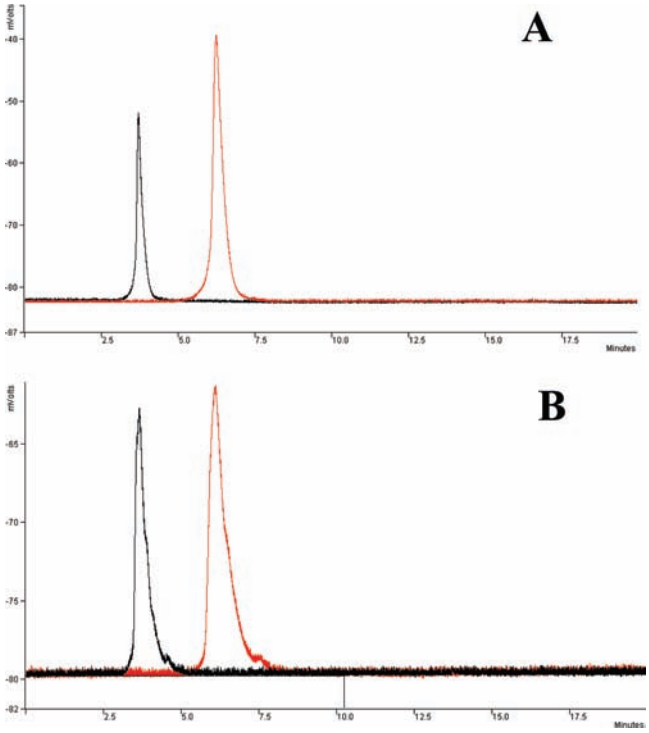

Figure 2. High performance liquid chromatograms using a silica column (150 mm × 4.6 mm with 5 μm particle size) and 6:3:1 mixture of ACN/H_2O/KNO_3 with 0.1% TFA and a flow rate of 0.4 mL/min. Injection volume is 5 μL. (A) $[Cu_2(\mathbf{3})_2]$ (black line) versus **3** (red line); (B) $[Cu_2(\mathbf{4})_2]$ (black line) versus **4** (red line).

neighboring protons on the aminoethyl glycine backbone. For example, in the COSY spectrum of compound **3**, the presence of the pyridine ligand is confirmed in both dipeptides by the presence of a peak corresponding to two protons at 7.1 ppm (Supporting Information, Figure S2, peak k) correlated to a second peak corresponding to the two protons at 8.4 ppm (Supporting Information, Figure S2, peak l). The terpyridine protons closest to the nitrogens ~8.8 ppm (Supporting Information, Figure S2, peak q) couple with their neighboring protons ~7.3 ppm (Supporting Information, Figure S2, peak p) and enabled the assignments for the other terpyridine protons in the COSY spectrum. The final two protons on the terpyridine rings located at 8.3 ppm (Supporting Information, Figure S2, peak m) in the 1D ^{1}H NMR spectrum exhibited no coupling in the COSY spectrum since these are electronically isolated. In contrast, the COSY spectrum of molecule **4** contains a peak corresponding to two protons at 7.9 ppm (Supporting Information, Figure S7, peak m) that couples with a second peak corresponding to two protons around 7.3 ppm (Supporting Information, Figure S7, peak n); these are assigned to the phenyl ring on the ligand. In both COSY spectra, there is correlation between the protons of the fmoc protecting group (4.1−4.4 ppm, Supporting Information, Figures S2 and S7 peaks e, f) and the bridging ethyl group (3.2−3.7 ppm, Supporting Information, Figures S2 and S7 peaks i, j, h, g). Taken together, the HMBC and HMQC spectra conclusively confirm the identity of the dipeptides.

Mass spectrometry was used for additional characterization of the dipeptides. High resolution molecular ion peaks were observed for dipeptide **3** ($(M + H)^+$ m/z: calculated 889.3969, found 889.4037) and dipeptide **4** ($(M + H)^+$: calculated 964.4339, found 964.4350) and further confirm their identities. Elemental analysis affirmed the purity of the two dipeptides, which were observed to be hygroscopic.

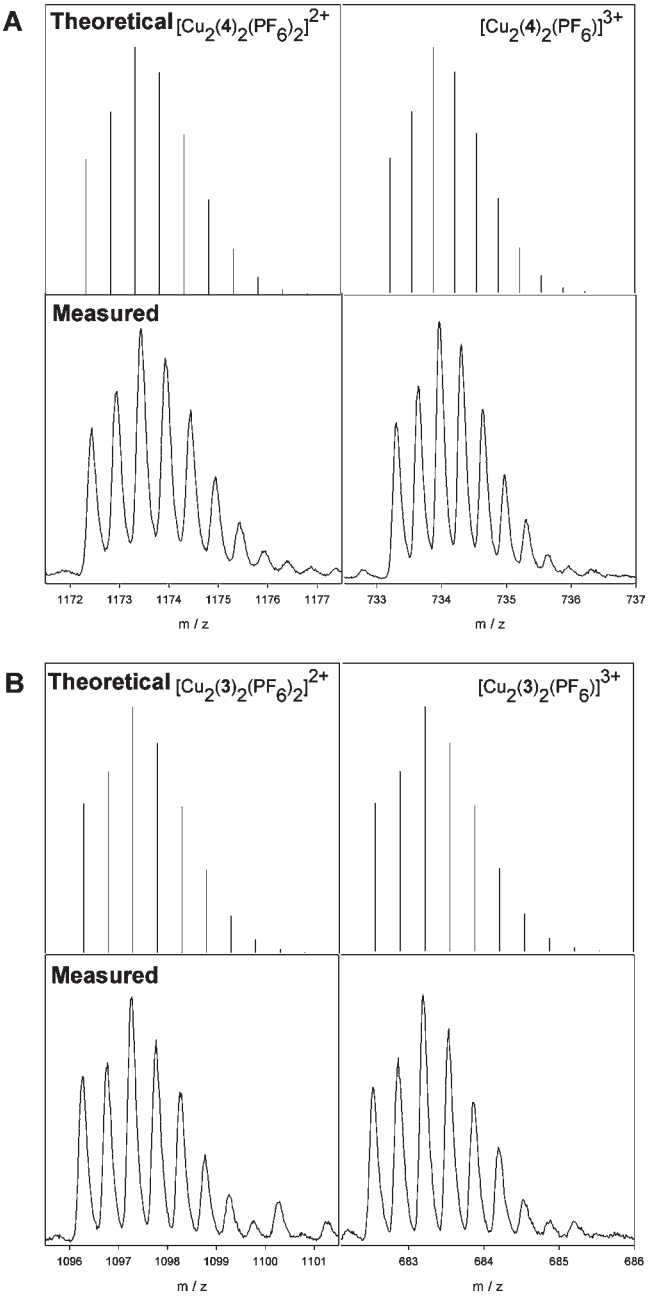

Figure 3. Positive ion electrospray mass spectra of (A) $[Cu_2(\mathbf{4})_2]^{4+}$ and (B) $[Cu_2(\mathbf{3})_2]^{4+}$, which are observed together with associated PF_6^- anions (as indicated). The theoretical isotope patterns for the +2 and +3 charged ions (containing two and one PF_6^- anion, respectively) are shown for comparison.

Synthesis and Characterization of Duplexes. Addition of Cu(II) to each dipeptide is expected to cause formation of $[Cu(py)(tpy)]^{2+}$ complexes, resulting in coordinative cross-links between the strands. To form the duplexes, the peptide strands must coordinate two metal ions and align in an antiparallel fashion, as in Figure 1B. Copper has initially been used for duplex self-assembly because it is sufficiently labile to allow the formation of

Table 1. UV-vis Absorbance Data for the Monomers and Dipeptides

molecule	$\lambda^{abs}{}_{max}{}^{a}$, nm ($\varepsilon$, 10^3 M^{-1} cm^{-1})
py monomer	264 (34.5), 278 (19.7)
tpy monomer (**2**)	276 (36.1), 300 (23.3)
Φ-tpy monomer	255 (60.1), 267 (65.2), 275 (66.1)
3	264 (34.3), 276 (33.7), 300 (20.3)
4	255 (53.7), 267 (56.8), 278 (57.7)

[a] Wavelength of the maximum absorbance of the peak.

the most thermodynamically stable structure to be obtained under mild heating. Addition of Cu(II) to a methanolic solution of the dipeptides while refluxing resulted in methanol-soluble product, which was then isolated by diluting the solution with water and precipitating the complex with ammonium hexafluorophosphate. To assess the purity of the resulting Cu-containing products, HPLC was used and the chromatograms compared to the unmetalated dipeptides; Figure 2 shows these chromatograms obtained under identical conditions. The individual chromatograms of dipeptides **3** and **4**, and those of the Cu(II)-containing products, contain a single, sharp peak. We note the presence of a small side peak in the chromatogram of both **4** and its Cu complex, but in such a low relative quantity that it represents a very minor impurity. Because the eluent (0.1% TFA in 6:3:1 ACN/H_2O/aqueous saturated KNO_3) is highly polar, in comparison with the pure peptides, the metalated products elute at an earlier time because of their greater charge.[18] In the chromatograms of the metalated dipeptides, we do not observe a peak at a time expected for pure dipeptide, and the peak widths are approximately the same for metalated versus unmetalated molecules. These HPLC data therefore confirm the presence of a single Cu-containing product following the reaction of Cu(II) with each of the dipeptides. Separate vapor pressure osmometry experiments of the Cu complexes in acetonitrile solutions provide molecular weights that are consistent with the dipeptide duplexes linked by two metal ions (2200−2900 g/mol), although imprecision in these values results in part from varying amounts of residual solvent present in the Cu complexes.

Therefore we employed positive ion electrospray mass spectrometry (ESI+ MS) to confirm the identities of the products. Using conditions for the mass spectrometric experiments from Gatlin et al.,[19] mass spectra were obtained as shown in Figure 3 (full spectra are shown in Supporting Information, Figures S14 and S15). Molecular ion peaks corresponding to the +2 and +3 duplexes were found for each of the metalated compounds with associated PF_6^- anions: the +2 peaks are identified as the species $[Cu_2(\mathbf{3})_2(PF_6)_2]^{2+}$ or $[Cu_2(\mathbf{4})_2(PF_6)_2]^{2+}$, whereas the +3 peaks are $[Cu_2(\mathbf{3})_2(PF_6)]^{3+}$ and $[Cu_2(\mathbf{4})_2(PF_6)]^{3+}$.[13b] These observed peaks confirm the duplex identities. Similar to our prior reports,[1] although the mass spectra are complex and a significant number of fragments are observed, we do *not* observe molecular ion peaks for higher order structures (e.g., $[Cu_n(peptide)_n(PF_6)_x]^{2n-x}$) or monometallic species (e.g., $[Cu(peptide)(PF_6)_x]^{2-x}$). Although it is possible that the former of these would likely be more difficult to ionize and therefore not appear in the mass spectra, it is important to note that only a single peak is observed in each of the chromatograms. For a single, higher order structure to form in solution and then decompose in the gas phase into only the $[Cu_2(peptide)_2]^{4+}$ structure (with associated anions), and not $[Cu(peptide)]^{2+}$ or $[Cu_3(peptide)_3]^{6+}$, etc.), is unlikely. Therefore, we use the sum of the data to conclude that even if higher order polymeric structures form in the reaction solution, these are present in extremely small quantities, are most likely insoluble and therefore not detected by HPLC or mass spectrometry, and the majority of the reaction product is the dipeptide duplex linked by two metal ions.

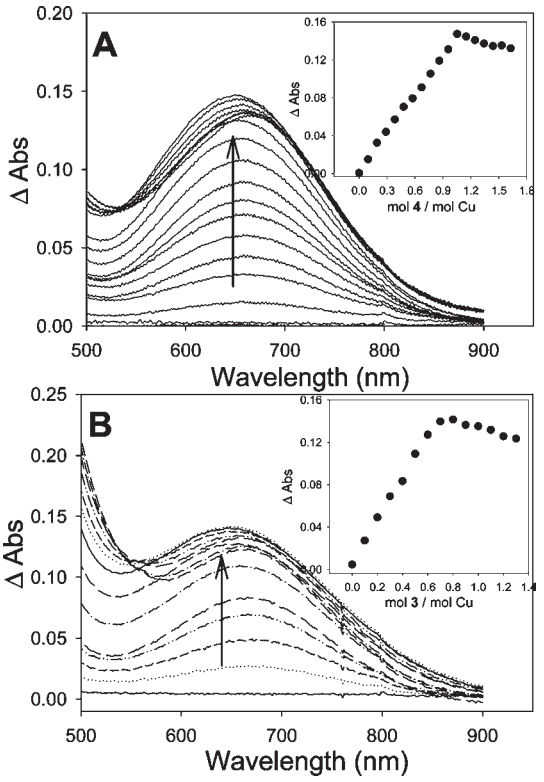

Figure 4. Spectophotometric titrations of the reaction of Cu^{2+} with dipeptides: (A) 7.64 mM dipeptide **4** titrated in 50 μL increments into a 2.0 mL volume of 1.91 mM $Cu(NO_3)_2$; and (B) addition of 50 μL increments of 9.55 mM dipeptide **3** into 2.0 mL of 1.91 mM of $Cu(NO_3)_2$. All solutions are in methanol. Insets: change in the absorbance at 650 nm as a function of the relative molar ratio of added peptide to Cu^{2+}.

Finally, we acquired ^1H NMR spectra of these compounds because the presence of Cu(II) results in a paramagnetic shift of the ligand protons to which it coordinates, and broadens nearby protons. An absence of ligand protons in the ^1H NMR spectra of $[Cu_2(\mathbf{3})_2]^{4+}$ and $[Cu_2(\mathbf{4})_2]^{4+}$ (Supporting Information, Figures S12 and S13) verified that the Cu(II) was coordinated to both py and tpy ligands (in **3**) or py and ϕ-tpy ligands (in **4**). Although the aminoethylglycine backbone is flexible, because of the short dipeptide length, the two ligands are spaced closely and are not able to coordinate to the same metal ion.[10a,b] The NMR results confirm that the Cu ion is not solely coordinated to the tridentate ligands, but also binds py close in its coordination shell. To accomplish this, the Cu ions must cross-link ligands on separate strands. Taken together, the HPLC, NMR, vapor pressure osmometry, and mass spectrometry data point toward the formation of the species

(18) Elliott, C. M.; Freitag, R. A.; Blaney, D. D. *J. Am. Chem. Soc.* **1985**, *107*, 4647–4655.
(19) Gatlin, C. L.; Turecek, F. *J. Mass Spectrom.* **2000**, *35*, 172–177.

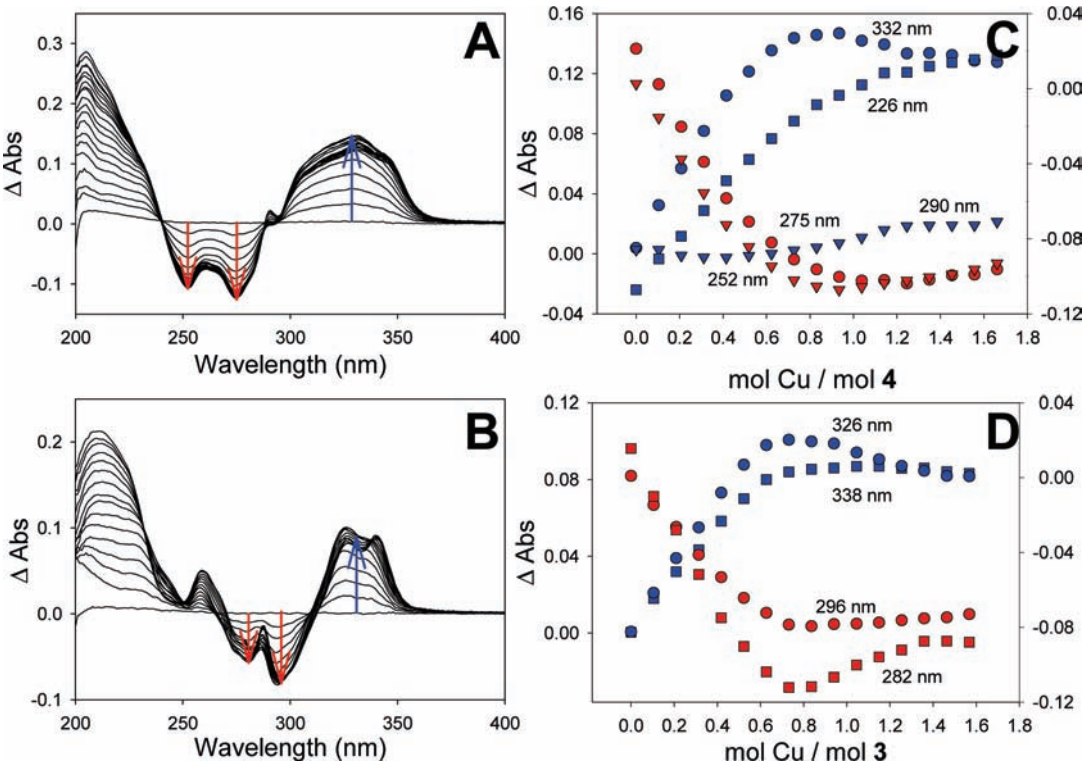

Figure 5. Difference spectra acquired during the spectophotometric titration of the reaction of Cu^{2+} with (A) 2.0 mL of 10 μM dipeptide **4**; and (B) 2.0 mL of 10 μM dipeptide **3** in methanol. Cu^{2+} is added in 50 μL increments of 40 μM of $Cu(NO_3)_2$. (C) and (D) are plots of the change in the absorbance at the indicated wavelength as a function of the relative molar ratio of added Cu^{2+} to **6** and **5**, respectively. Blue symbols correspond to ΔA values on left axis; red symbols on right axis.

containing two dipeptides cross-linked by two metal ions, as depicted in Figure 1B.

Metal Coordination to Dipeptides

The above experiments demonstrated the self-assembly of the di-Cu linked dipeptide duplexes. To begin to understand how these structures form in the presence of copper, a series of spectrophotometric titrations were also performed. Dipeptides **3** and **4** were first studied using UV−visible spectrophotometry to give quantitative measures of their extinction coefficients (Table 1). The UV−vis spectra of the nonmetallated dipeptides are dominated by absorbances due to the $\pi_{tpy}-\pi^*_{tpy}$ and the $\pi_{\phi\text{-}tpy}-\pi^*_{\phi\text{-}tpy}$ transitions at 260−310 nm in **3** and 240−290 nm in **4**, respectively, which are consistent with other terpyridine and phenyl terpyridine systems.[20] The pyridine ligand also has a $\pi_{py}-\pi^*_{py}$ transition absorbance at 264 nm, but it is not easily identified because this region of the spectrum contains many overlapping peaks. Upon Cu(II) coordination to the dipeptides, the $\pi-\pi^*$ absorption bands of the ligands shift to 310−350 nm, and a band appears in the visible region at ~650 nm.

Spectrophotometric titrations at higher concentrations were performed so that the low energy transition (650 nm) could be monitored. Figure 4 contains the difference spectra obtained during the titration of compounds **3** or **4** into a solution containing Cu(II). Since neither dipeptide absorbs light in this region of the visible spectrum, this peak is assigned to the d-d transition of the resulting Cu complex.[10b] In the Figure 4 insets, plots of the incremental change in absorbance at the peak maxima are plotted versus the relative ratio of peptide to Cu, and show an increase in absorbance as dipeptide is added. In the case of **4**, the maximum absorbance occurs at a mole ratio of ~1:1 dipeptide/Cu and then slightly decreases. In contrast, the titration curve of **3** in Figure 4A has a maximum absorbance at ~0.75 Cu/dipeptide and falls with additional aliquots of dipeptide. These stoichiometric points are consistent with either a single Cu coordinated to a single dipeptide, or two Cu ions linking two dipeptide strands. Because of the steric hindrance imparted by the close proximity of the two ligands on each strand, and using our understanding of the products of the dipeptide reactions with Cu (vide supra), we conclude from these data that the $[Cu_2(peptide)_2]^{4+}$ structures are formed at the ~1:1 stoichiometric point. In the Cu titrations of both **3** and **4**, we hypothesize that the decrease in absorbance after this stoichiometric point to formation of $[Cu(tpy)]^{2+}$ and $[Cu(py)]^{2+}$ complexes at the expense of metal-linked duplex. That is, addition of extra ligand shifts the equilibrium from $[Cu(tpy)(py)]^{2+}$ to (primarily) [Cu(tpy)] and [Cu(py)]; the later occurrence in the titration curve of **4** suggests that this Cu-linked duplex is more stable than for **3**, and therefore larger amounts of Cu(II) are required to dis-associate the structure. Ongoing experiments aim to specifically measure association constants and stabilities.

Using lower concentrations to examine the UV region of the spectrum provides insight into the changes observed ligand-centered transitions, and approaches the complexation equilibria from the opposite direction. Separate titrations of Cu(II) into solutions of the dipeptides reveal isosbestic points at 270 and 310 nm for reaction with **3**, and at 240 and 290 nm for reaction with **4**. The difference spectra

(20) Araki, K.; Arita, S.; Cheon, J.-D.; Mutai, T. *J. Chem. Soc., Perkin Trans.* **2001**, *2*, 1045–1050.

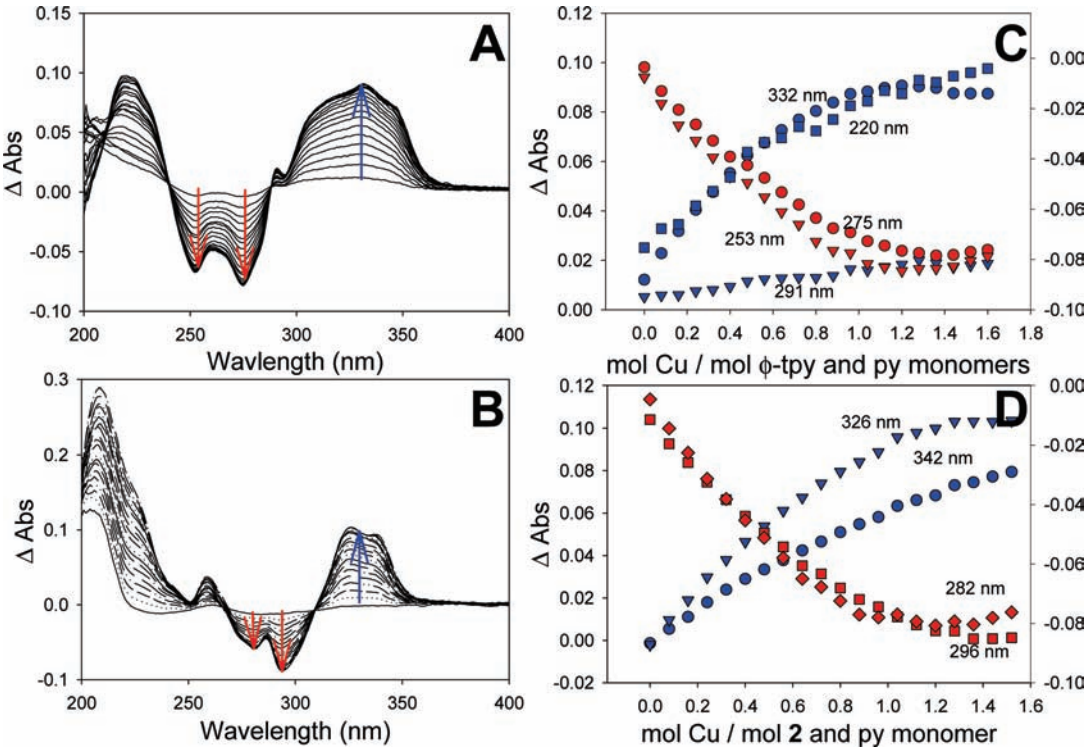

Figure 6. Titration of a 2.0 mL methanolic solution containing (A) 10 μM fmoc-aeg(py)-OH and 10 μM **2** and (B) a 2.0 mL solution containing 10 μM fmoc-aeg(py)-OH and 10 μM fmoc-aeg(ϕ-tpy)-O*t*Bu, with 25 μL increments of 50 μM of $Cu(NO_3)_2$. Plots of the change in absorbance at the indicated wavelengths as a function of the relative molar ratio of added Cu^{2+} to peptides: (C) fmoc-aeg(py)-OH and **2**; (D) fmoc-aeg(py)-OH and fmoc-aeg(ϕ-tpy)-O*t*Bu . Blue symbols correspond to ΔA values on left axis; red symbols on right axis.

in Figure 5 show that as Cu(II) is added to the solution of dipeptide, the absorbance of the free ligand decreases and a concomitant increase in the metal-coordinated ligand absorbance is observed. Plotting the intensity of the new absorbance peak versus the molar ratio of Cu(II) to dipeptide results in the titration plots shown in Figures 5C and D which increase and reach a constant absorbance at a ~1:1 ratio of Cu/dipeptide. This stoichiometric ratio is again associated with two Cu ions linking two dipeptides. At select wavelengths, the absorbance continues to vary beyond the duplex stoichiometric point as additional Cu^{2+} is added, consistent with the hypothesis that beyond this point other complexes (e.g., $[Cu(tpy)(H_2O)]^{2+}$ and $[Cu(py)(H_2O)_3]^{2+}$) could be forming.

For comparison, spectrophotometric titrations of Cu(II) into solutions containing *unlinked* ligand-modified aeg monomers at the identical concentrations to the experiments in Figure 5 were also performed, and these are shown in Figure 6. The difference spectra acquired for these titrations contain isosbestic points at the same wavelengths as the dipeptide counterparts (Figure 5). Decreasing absorbance is observed at wavelengths associated with unmetalated ligand in both Figures 5C and D and 6C and D as the ligands coordinate to Cu(II). Concomitant absorbance increases are observed at new wavelengths that are attributed to metal complex formation. Comparison of the extinction coefficients (ε) obtained for the unlinked ligands versus metalated dipeptide is listed in Table 2. These data show that ε is approximately twice as large in the Cu-containing dipeptide, indicative of two Cu centers per dipeptide duplex.

The titration plots in Figures 6 C and D have an inflection point, suggesting a similar bonding motif of Cu(II) with the ligands (e.g., $[Cu(py)(tpy)]^{2+}$). However, when the monomers are unlinked, the rise of the titration curve is shallower than in Figure 5, and the inflection point occurs beyond the expected 1:1 molar ratio of Cu to dipeptide. This result suggests a higher binding affinity when the ligands are tethered on the dipeptide, consistent with positive cooperativity. Because of the extensive overlap and complexity of the absorbance spectra, continuing studies are underway to quantify the apparent cooperative effects and binding affinities during formation of the dipeptide duplexes. In addition to quantitatively understanding the association constants for the formation of the metal-linked duplexes, our longer term objectives include examining the role of artificial peptide length on stability, and testing the specificity and selectivity of recognition between strands analogous to sequence-specific DNA hybridization.

Table 2. UV-vis Absorbance Data for Cu Complexes

complex	$\lambda^{abs}{}_{max}{}^{a}$, nm ($\varepsilon$, 10^3 M^{-1} cm^{-1})
$[Cu(py)(tpy)]^{2+}$	282 (30.8), 326 (15.0), 338 (14.1)
$[Cu_2(\mathbf{3})_2]^{4+}$	282 (43.7), 326 (28.5), 338 (24.7)
$[Cu(py)(\Phi\text{-tpy})]^{2+}$	275 (61.5), 290 (53.6), 332 (24.6)
$[Cu_2(\mathbf{4})_2]^{4+}$	275 (74.5), 290 (84.8), 332 (47.5)

[a] Wavelength of the maximum absorbance of the peak.

Acknowledgment. We gratefully acknowledge support of this work by a grant from the National Science Foundation (CHE-0718373). We thank Megan Andes and Christine Keating for assistance with the vapor pressure osmometry measurement.

Supporting Information Available: Complete ^{13}C NMR of the tpy monomer, ^{1}H NMR, COSY, HMBC, HMQC spectra, and mass spectra of the dipeptides and Cu-linked duplexes. This material is available free of charge via the Internet at http://pubs.acs.org.